Proceedings of the ASME 2011 International Mechanical Engineering Congress & Exposition
IMECE2011
November 11-17, 2011, Denver, Colorado, USA

IMECE2011-64699

SEMI-AUTONOMOUS COLLABORATIVE CONTROL OF MULTI-ROBOTIC SYSTEMS FOR MULTI-TASK MULTI-TARGET PAIRING

Yushing Cheung
Department of Mechanical Engineering,
Stevens Institute of Technology,
Castle Point on Hudson,
Hoboken, NJ 07030, USA
Email: johnyscheung@gmail.com

Jae H. Chung & Ketula Patel
Network Lethality & Intelligent Systems,
US Army RDECOM-ARDEC,
Building 95N,
Picatinny Arsenal, NJ 07806, USA
Email: jae.chung3 & ketula.patel@us.army.mil

ABSTRACT

In many applications, it is required that heterogeneous multi-robots are grouped to work on multi-targets simultaneously. Therefore, this paper proposes a control method for a single-master multi-slave (SMMS) teleoperator to cooperatively control a team of mobile robots for a multi-target mission. The major components of the proposed control method are the compensation for contact forces, modified potential field based leader-follower formation, and robot-task-target pairing method.

The robot-task-target paring method is derived from the proven auction algorithm for a single target and is extended for multi-robot multi-target cases, which optimizes effect-based robot-task-target pairs based on heuristic and sensory data. The robot-task-target pairing method can produce a weighted attack guidance table (WAGT), which contains benefits of different robot-task-target pairs.

With the robot-task-target pairing method, subteams are formed by paired robots. The subteams perform their own paired tasks on assigned targets in the modified potential field based leader-follower formation while avoiding sensed obstacles. Simulation studies illustrate system efficacy with the proposed control method.

INTRODUCTION

Cooperative control of multi-robotic systems has been studied extensively in recent years [5, 7, 8, 11–13, 15–17], especially for some tasks that cannot be handled by one single robot. It can improve dexterity of robots and enlarge application fields of robots. Thus, many cooperative control algorithms have been proposed so far [5, 7, 8, 11–13, 15–17]. There are two types of cooperation. One is the cooperation without force interactions among robots (unconstrained motion tasks) and the other is with them (constrained motion tasks). In the former type of cooperation, task planning is one of the main technical problems, but the same positional controller as that of single robot can be used and it can be realized very easily. Therefore, this type of cooperation has been practically used for target captures or enclosure [5, 12, 15, 17]. In the latter type of cooperation, under the interactions of forces, design of the control strategies, which can keep inner forces between robots to be desired values and also ensure the stability of the controllers, becomes the most critical problem. This has been seen for target transportations as the force or impedance controller has been commonly used [7,8,16]. Besides these two types of cooperation, the transition between them has been investigated in some papers [11, 13]. The transition involves a smooth, stable switching between motion and force control when instability and large force spikes during the switching are avoided. However, in those papers [11, 13], a control method was not developed to split a robot team into several sub-teams to do the different motion tasks when applications, such as military operation, space exploration, and etc. request all robots to do the multi-motion tasks simultaneously.

Furthermore, in many applications, unstructured nature of the worksite environments and the limitations of the current sensors and computer decision-making technologies prohibit the use of fully autonomous systems for the operations [6, 8]. Therefore, it is required that the human decision making be involved in the

Report Documentation Page

Form Approved
OMB No. 0704-0188

1. REPORT DATE	2. REPORT TYPE	3. DATES COVERED
NOV 2011		**00-00-2011 to 00-00-2011**

4. TITLE AND SUBTITLE	5a. CONTRACT NUMBER
Semi-Autonomous Collaborative Control of Multi-Robotic Systems for Multi-Task Multi-Target Pairing	5b. GRANT NUMBER
	5c. PROGRAM ELEMENT NUMBER
6. AUTHOR(S)	5d. PROJECT NUMBER
	5e. TASK NUMBER
	5f. WORK UNIT NUMBER
7. PERFORMING ORGANIZATION NAME(S) AND ADDRESS(ES) **US Army RDECOM-ARDEC,Network Lethality & Intelligent Systems,Building 95N,Picatinny Arsenal,NJ,07806**	8. PERFORMING ORGANIZATION REPORT NUMBER
9. SPONSORING/MONITORING AGENCY NAME(S) AND ADDRESS(ES)	10. SPONSOR/MONITOR'S ACRONYM(S)
	11. SPONSOR/MONITOR'S REPORT NUMBER(S)

12. DISTRIBUTION/AVAILABILITY STATEMENT
Approved for public release; distribution unlimited

13. SUPPLEMENTARY NOTES

14. ABSTRACT

In many applications, it is required that heterogeneous multirobots are grouped to work on multi-targets simultaneously. Therefore, this paper proposes a control method for a singlemaster multi-slave (SMMS) teleoperator to cooperatively control a team of mobile robots for a multi-target mission. The major components of the proposed control method are the compensation for contact forces, modified potential field based leaderfollower formation, and robot-task-target pairing method. The robot-task-target paring method is derived from the proven auction algorithm for a single target and is extended for multi-robot multi-target cases, which optimizes effect-based robot-task-target pairs based on heuristic and sensory data. The robot-task-target pairing method can produce a weighted attack guidance table (WAGT), which contains benefits of different robot-task-target pairs. With the robot-task-target pairing method, subteams are formed by paired robots. The subteams perform their own paired tasks on assigned targets in the modified potential field based leader-follower formation while avoiding sensed obstacles. Simulation studies illustrate system efficacy with the proposed control method.

15. SUBJECT TERMS

16. SECURITY CLASSIFICATION OF:			17. LIMITATION OF ABSTRACT	18. NUMBER OF PAGES	19a. NAME OF RESPONSIBLE PERSON
a. REPORT	b. ABSTRACT	c. THIS PAGE			
unclassified	**unclassified**	**unclassified**	**Same as Report (SAR)**	**10**	

systems. Teleoperators, in which a human operator is an integral part of the control, are established to integrate the human decisions to the control loop of the systems. By minimizing the required human resources and amplifying the human effort, the single-master multi-slave (SMMS) teleoperation has been considered in this paper.

Fong et. al. suggested the collaborative control with dialogue functions to remotely operate the multi-robot via a master robot to search in an open area [5]. With their approaches, the slave robots have more freedom in execution and are more likely to find a good solution by themselves when they have a problem. The human operator is able to function as a resource for the slave robots, providing information and processing just like other system modules. Nevertheless, their framework for coordination does not contain any mechanism for remotely regrouping the team robots into several sub-teams to carry out multi-tasks containing unconstrained and constrained motions to capture and transport multi-targets simultaneously.

Many different methods to assign multi-tasks and multi-targets to subteams have been widely applied in fully automatic coordinated multi-robotic systems [10]. The methods are a genetic or improved genetic algorithm [3], ant colony system [9], particle swarm optimization [10], market-based approaches [4], and auction or decentralized cooperation auction [14]. Nonetheless, they have no ability to stably converge to a global optimum. Therefore, Bogdanowicz and Coleman et. al. recommended a method for optimization of effect-based weapon-target pairings [1] to decide a preferred weapon-target combination for engaging a given target by scanning attack guidance tables. Different from those previously mentioned methods, it is a rule and function based, not an optimized method. Therefore, it can converge rapidly and produce a suboptimal solution stably. Nonetheless, Bogdanowiczs and Colemans optimization was only focused on matching several weapon combinations with numerous targets in a single-motion task, which could not fit into a general mission with multi-motion tasks.

Due to the above mentioned problems, the primary objective of this paper is to develop a control method for a SMMS teleoperator to cooperatively control a team of heterogeneous mobile robots for robot-task-target pairing. Primary components of the proposed control method are (1) modified potential field based leader-follower formation, (2) compensation for contact forces [2], and (3) robot-task-target pairing. During the operation, the human operator only focuses on controlling a team leader robot. All other team robots autonomously make a formation regarding its positions and velocities based on sensory information. Therefore, the formation is adapted by modifying their paths for obstacle avoidance by using the modified potential field based leader-follower formation controller developed in our research papers [2]. Moreover, in the constrained motion, the compensator for the contact forces enables the slave robots to adapt their forces acting on the transported target to have a firm grip of it. When the team leader is close to targets, the team robots are assigned tasks and targets correspondingly with the robot-task-target pairings, and then the subteams are formed based on optimal robot-task-target pairs. In addition, the subteam leaders are selected based on robot functionalities and proximity to the targets to lead the subteams.

The rest of this paper is organized as follows. In Section 2, the control method that integrates the primary components to execute different motion tasks simultaneously with different subteams for a robot-task-target approach is proposed. In Section 3, the effectiveness of the task achievement of the SMMS system with the proposed control method were evaluated through simulation studies. Section 4 concludes this paper and shows future research directions.

SEMI-AUTONOMOUS SINGLE-MASTER MULTI-SLAVE (SMMS) TELEOPERATION CONTROL METHOD FOR A ROBOT-TASK-TARGET APPROACH

This paper extends the preliminary concepts of the semi-autonomous SMMS teleoperation control method [2] which was only focused on a single-target into a multi-target operation, i.e. several simultaneous target captures and transportations, in a complicated environment. The major difference for cooperative robots between completion of the multi-task and single-task is a robot-task-target pairing method.

In this paper, we develop the robot-task-target pairing method to make the semi-autonomous SMMS teleoperation control method proposed in [2] be able to deal with the multi-task on the multi-target. The detail of the robot-task-target pairing method mentioned above is formulated in the following subsection.

Robot-Task-Target Pairing Method

Consider such a scenario, in a two-dimensional and limited rectangular environment X with n_c square cells, n_p slave robots pursue n_e targets, for $n_p > n_e$. The set of the robots is denoted by a matrix of $A = [a_1, a_2, ...a_{n_p}]$ where a_j is the j^{th} robot matrix. The j^{th} robot capability vector for the t^{th} task is denoted by $\hat{C}_j^t$, $1 \leq j \leq n_p$, and the set of targets is expressed as a target matrix of $T = [T_1, T_2, ...T_{n_e}]$ where T_{ne} is the ne^{th} target matrix. The vector representing the capability required to accomplish the t^{th} task on the T^{th} target is denoted by $\bar{C}_t^T$, $1 \leq T \leq n_e$. Agent $A \cup T$ denotes the teams of robots and targets. For simplification, we assume that both space and time can be quantized, therefore the environment can be regarded as a finite collection of cells, denoted by $X_c = 1, 2, ..., n_c$. There exist some static obstacles with fixed sizes and regular shapes, and their locations are determined by the mapping $m : X_c \rightarrow 0, 1$, for $\forall x \in X_c, M(x) \geq thresh1$ indicates that the cell x is occupied by obstacles. $\forall x \in X_c, M(x) \leq thresh2$ indicates that the cell x is free, where $thresh2 < thresh1$ represents the threshold value between 0 and 1. Each of the het-

erogeneous team robots needs different capabilities to complete different tasks on different targets, such as the target capture and transportation.

Robot Capability

For the t^{th} task, j^{th} robot, and $1 \leq m \leq u$, the weighted capability vectors of the j^{th} robot to complete the i^{th} task can be defined as

$$\hat{C}_j^t = w_j^T diag\{b_{j1}^t, b_{j2}^t, ..., b_{ju}^t\} \left[c_{j1}^t \ ..... \ c_{jm}^t\right]^T \qquad (1)$$

where u is the maximum number of the vectors, each of which represents the individual functionality. All heterogeneous robots are represented by the set of robot matrices, e.g. $A = \begin{bmatrix} a_{11} & a_{12} & a_{13} & ..... & a_{1r} \\ a_{21} & a_{22} & a_{23} & ..... & a_{2r} \\ ..... & ..... & ..... & ..... & ..... \\ a_{n_v1} & a_{n_v2} & a_{n_v3} & ..... & a_{n_vr} \end{bmatrix}$ where n_v, for $0 < n_v \leq n_p$, is the total number of the robots in the team, and r, for $0 < r \leq n_e$, is the total number of the tasks. c_{jk}^t is a capability vector for the k^{th} functionality and the t^{th} task. w_j^T is a positive integer such that for the given target T and robot j, the following is satisfied. If the robot is assigned to the target, $w_j^T = 0$, otherwise, $w_j^T = 1$. The $u \times u$ dimension diagonal matrix of b_{ju}^t is used to estimate the percentage of possibility of using the $u \times 1$ dimensional capability vector C_j^t to do the t^{th} task by the j^{th} robot successfully. However, if the j^{th} robot does not have the capability c_{jk}^t, then the b_{jk}^t is 0. Each robot matrix in A has more than one weighted capability vector, e.g. for the j^{th} robot and t^{th} task, $a_{jt} = [\hat{C}_j^t]^T$.

Capability Required to Execute Tasks on Targets

It is assumed that there are p tasks which need to be done independently and simultaneously. All tasks are represented by a set of task matrices e.g. $t = \{t_1, ...t_p\}$ in the system for $p \leq n_e$, i.e. one task can be paired to two or more targets, but each target can only be paired to one task. The capability vector that is required to accomplish the t^{th} task on the T^{th} target is defined as

$$\bar{C}_t^T = diag\{\beta_{t1}^T, \beta_{t2}^T, ..., \beta_{tu}^T\} C_{tu} \qquad (2)$$

where the $u \times u$ dimension diagonal matrix of β_{tu}^T is used to describe the percentage of possibility of using the $u \times 1$ dimension capability vector C_{tu} with which the robot can finish the t^{th} task on the T^{th} target. $C_{tu} = [c_{t1}.....c_{tu}]^T$ when the total number of the functionalities is u. c_{tu} is the capability vector that is required to complete the t^{th} task with the u^{th} functionality. However, if the t^{th} task can not be done successfully by any robot with the capability C_{tu} on the T^{th} target, then the β_{tu}^T is 0. Otherwise, β_{tu}^T is 1.

Subteam Capability

The subteam is a combination of the multi-robots that work on the t^{th} task cooperatively. For the j^{th} robot, t^{th} task, and $a_{jt} > 0$, $u_{(a,b)} = a_{jt}$ for $p \geq b \geq 1$ and $a_{max} \geq a \geq a_{min}$, $a_{min} \geq 1$, and $a_{max} \leq n_p$ where $n_p/(a_{max} - a_{min} + 1) = n_s$ where n_s is the total number of subteams. The y^{th} subteam is represented by the matrix of $D_y = \begin{bmatrix} u_{(a_{min},1)} & ..... & u_{(a_{max},1)} \\ u_{(a_{min},2)} & ..... & u_{(a_{max},2)} \\ ..... & ..... & ..... \\ u_{(a_{min},r)} & ..... & u_{(a_{max},r)} \end{bmatrix}$, because the robot team denoted by A can be formed by several subteams, one of which is denoted by D_y, i.e. $A = \{D_1, D_2, .., D_y, .., D_q\}$ where q is the total number of the combinations of multi-robots (robot subteams) in the robot team. For the j^{th} robot and t^{th} task, if $\hat{C}_j^t > 0$, then

TABLE 1: Weighted Attack Guidance Table (WAGT)

Subteam 1	$m_{N,1}$	$\cdots$	Subteam n	$m_{N,n}$
$B_{11}^1, \ldots, B_{x1}^1$	$m_{1,1}$	$\cdots$	$B_{1n}^1, \ldots, B_{xn}^1$	$m_{1,n}$
$B_{11}^2, \ldots, B_{x1}^2$	$m_{2,1}$	$\cdots$	$B_{1n}^2, \ldots, B_{xn}^2$	$m_{2,n}$
.....	...	...	.....	...
$B_{11}^N, \ldots, B_{x1}^N$	$m_{N,1}$	$\cdots$	$B_{1n}^N, \ldots, B_{xn}^N$	$m_{N,n}$

$$Q_{(i_a,t)} = \hat{C}_j^t \quad for \quad n_p \geq i_a \geq 1 \qquad (3)$$

where the $Q = \left[Q_{(1,t)} \ \cdots \ Q_{(n_p,t)}\right]$ is a positive integer. The y^{th} subteam capability vector for the t^{th} task is defined as

$$\tilde{C}_{(y_a:y_b,t)}^y = \sum_{i_a=y_b}^{i_a=y_a} Q_{(i_a,t)} \qquad (4)$$

where $y_b - y_a, \forall y_b \geq y_a$, is the total number of the robots in the y^{th} subteam. y_a is the first and y_b is the last indices of the elements in the matrix $Q_{(i_a,t)}$ for the given task t and the y^{th} subteam. The y^{th} subteam is able to perform the t^{th} task on the T^{th} target if the condition, $\bar{C}_t^T \leq \tilde{C}_{(y_a:y_b,t)}^y$, is satisfied. The subteam leader is selected when its magnitude of the capability vector $\hat{C}_j^t$ is largest among the others in the same subteam. The subteam leader knows all capability information about its subteam members.

Bidding Winner Determination

In Table 1, $m_{N,n}$ is the positive integer weight for the n^{th} subteam to bid on the x^{th} task and N^{th} target. If $\tilde{C}_{(y_a:y_b,x)}^n$ is smaller than the base price which is a positive integer, or the N^{th} target has already been assigned to the n^{th} robot subteam, $m_{N,n}$ is 0. Otherwise, $m_{N,n}$ is 1. By arranging $m_{N,n}$ and B_{xn}^N into Table 1, called Weighted Attack Guidance Table (WAGT), each row of WAGT corresponds to a target with Tasks (1 to x) and Robot

Subteam (1 to n) when x is the total number of the tasks, and n is the total number of the subteams formed in the team. In addition, each column of WRT corresponds to a robot combination (Robot Subteam) that accomplishes Tasks (1 to x) on Targets (1 to N) when N is the total number of the targets. Therefore, there are the N rows and n columns in WRT. The scanning proceeds from the first to the last column. Hence, the robot combination (Robot Subteam) specified in column i takes precedence over combination of robots specified in column $i+1$. From Table 1, for the n^th subteam and N^{th} target, the subteam bid matrix can be formed, i.e. $\tilde{B}(N,n) = \left[B^N_{1n}\ B^N_{2n}\ B^N_{3n}\ \ldots\ B^N_{xn} \right]$. The maximum value of the element in the matrix of $\tilde{B}(N,n)$ is the bid value for the task which is preferred to be done on the N^{th} target by the n^{th} subteam. For example, for the y^{th} subteam and k^{th} target, the bid value is weighted as follows.

$$\hat{B}(k,y) = \sum_{t=1}^{t=s_g} ((\tilde{C}^y_{(y_a:y_b,t)} - \bar{C}^T_t)(1 - X^k_{ty})) \tag{5}$$

where X^k_{ty} is the positive integer weight for the y^{th} subteam to do the k^{th} target. If the t^{th} task is the most preferred by the y^{th} subteam to be done on the k^{th} target when B^k_{ty} is the maximum value of the element in the matrix of $\tilde{B}(k,y)$, then $X^k_{ty} = 0$. Otherwise, $X^k_{ty} = 1$. The target bid matrix can be created, i.e. $\hat{B}^k = \left[\hat{B}(k,1)\ \ldots\ \hat{B}(k,n) \right]$ for the k^{th} target. Therefore, based on the given subteams, targets, tasks, WAGT, and optimization of the robot-task-target pairing that is described below, the bidding winner determination is made.

The optimization of the robot-task-target pairing is formulated as follows. Given the robot subteam y, targets T, tasks t, and WAGT, an assignment of the subteam is found in such a format that WAGT is satisfied, and its corresponding objective function in Eq. (6) is maximized within the given constraints in Eq. (7). Therefore, we can state the optimization problem as follows. For Target k and Subteam $1-n$ as seen in Table 1, the objective function is $ObjFun(k) = \left[(\hat{B}(k,1)m_{k,1})\ \ldots\ (\hat{B}(k,n)m_{k,n}) \right]$

$$maximize \quad ObjFun(k) \tag{6}$$

Subject to

$$\sum_{y=1}^{y=n} \hat{B}(k,y) \geq 0 \tag{7}$$

where $m_{k,y}$ is the positive integer weight for the y^{th} subteam and the k^{th} target. Initially, all $m_{k,y}$ is equal to one if no subteam is assigned to any target. However, if Subteam S is assigned to Target T, $m_{S_i,T}$ is equal to zero $\forall\ S_i \neq S$. Hence, Subteam S that proposes the maximum affordable value $(\hat{B}(T,S)m_{T,S})$ can win Target T by solving Eqs (6) within the constraints Eq. (7). By using the robot-task-target pairing method, the subteam/task/target pairs are stored into the resulted matrices e.g. the pair matrices and given WAGT. In order to split its team into some subteams to execute different tasks on different targets simultaneously, our proposed control method in [2] is modified into the system with the robot-task-target pairing method. The robot-task-target pairing method is created to enable the system based on the found pairs to form subteams, appoint the robots as a subteam leader and followers, pair the tasks to the subteams, and generate the position and force reference inputs to the subteams to work on the given targets. The other components of the proposed control method, e.g. the modified potential field based leader-follower formation and the contact force compensators, are similar to those in [2].

SMMS Teleoperator with the Proposed Modifications

The SMMS teleoperator with integrating the above mentioned control methods are modified into Figure 1. Figure 1 represents the overall architecture of the modified teleoperation system. The master and slave subsystems in Figures 1a and 1b, respectively, are connected over the wireless internet. The master subsystem is the same as the one in our papers [2]. The difference from the one in [2] is that the slave subsystem with the proposed control methods is operated fully autonomously for two reasons. (1) Human commands via the master subsystem are temporarily not available due to intermittently disrupted or delayed transmission between the subsystems. (2) The team formed by the slave robots is divided into the subteams to simultaneously perform the task on the target when the subteam robots are successfully paired to the proper tasks and targets with the robot-task-target pairing method. The modified system shown in Figure 1 is formulated into the following equations of motion.
Master:

$$M_m\ddot{e}_m + B_m\dot{e}_m + K_m e_m = 0 \tag{8}$$

i^{th} Slave:

$$M_{si}\ddot{e}_{si} + B_{si}\dot{e}_{si} + K_{si}e_{si} = U_T + U_o + (1-\sigma)(1-\lambda)U_f + C_e\delta F_{si} \tag{9}$$

where U_f is the virtual bonding between robots. U_T is the virtual attraction to the target while U_o is the virtual repulsion from the obstacles. C_e is the force compensator to regulate the contact

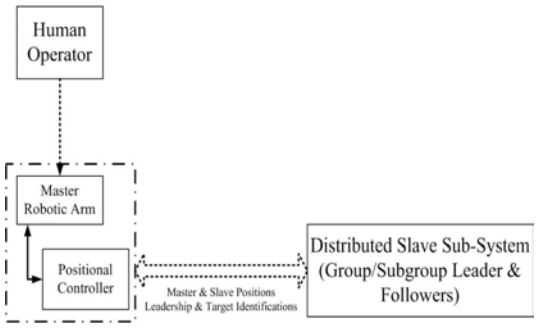

(a) Master subsystem

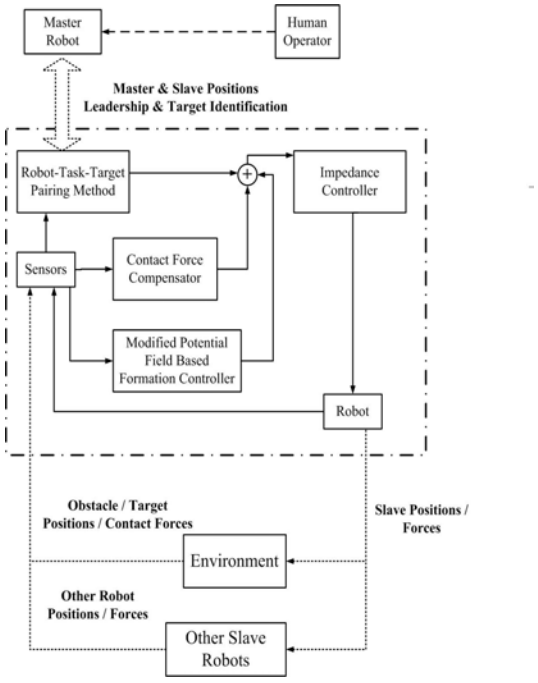

(b) Slave subsystems (leader/followers)

FIGURE 1: Modified SMMS Systems

force acting against the target to make a firm grip. U_f, U_T, U_o, and C_e were proposed in [2]. x_m and x_{si} are the master and the i^{th} slave robot position vectors, respectively. x_{sdi} is the reference position vector of the i^{th} slave robot. M_m is the inertia matrix of the master robot. K_m is the control parameters for the linear diagonal master matrices. M_{si} is the inertia matrices of the i^{th} slave robots. B_{si} is the slave impedance matrix. K_{si} is the control parameters for the linear diagonal slave matrices. σ and λ are the control parameters of the i^{th} slave robot. When the robot is selected as a team leader, σ is turned into one; otherwise, it becomes zero. When the robot is appointed as a subteam leader, λ becomes one; otherwise, λ is zero. B_m is the master adaptive impedance

TABLE 2: SMMS simulations for a multi-target mission

Sims	Robot Types	Control Objectives
Sim (1)	Homogeneous Robots	Non-Robot-Task-Target Pairing
Sim (2)	Homogeneous Robots	Robot-Task-Target Pairing
Sim (3)	Heterogeneous Robots	Robot-Task-Target Pairing

matrix. $e_{si} = x_{si} - (\sigma x'_m + (1-\sigma)X'_{ideal})(\alpha_1 + (1-\alpha_1)\psi_{pos})$. $e_m = x_m - x_h$, where x_h is the position vectors commanded by the human operator. x_{si} is the slave current robot positions. $\alpha_1 = |sgn(e_{si}^2)|$, which is the constant positive integers switching between zero and one in order to determine the output of the target matrix. ψ_{pos} is the matrix, $[0\ 0\ 1]^T$ to produce its reference position vectors transformed from X'_{ideal} x'_m and x'_{si} are the delayed transmitted x_m and x_{si}, respectively. X_{ideal} is the slave subteam robot reference position vectors. $\delta F_{si} = F_{si} - F_{ideal}(1-\alpha_1)\psi_{force}$ is a difference between reference and measured forces of the slave robots when F_{ideal} is the reference force vectors and F_{si} is the measured forces of the slave robots. ψ_{force} is the matrix, $[0\ 1\ 0]^T$ to produce its reference force vectors transformed from F'_{ideal} The slave team leader is remotely controlled by the human operator to guide the team. As mentioned above, when the team is approaching the targets, it is autonomously split into subteams paired to tasks and targets with the robot-task-target pairing method by solving Eqs (6) within the constraint, Eq. (7). Robot-task-target matrices are generated using Eqs (6) and transformed into the reference positions and forces for the robot to accomplish the assigned tasks on the assigned targets. Furthermore, during navigation to the assigned target, the subteam leader-follower formation is maintained or distorted by integrating (1) the virtual robot-robot bondings with different strengths based on which two team robots are connected, (2) the attraction to the target with regard to robot-target distances, and (3) the repulsion from the obstacles with regard to robot-obstacle distances. In such a formation, all followers in the subteam move with regard to the subteam leader's motion. After the target is reached, the slave robots will perform the assigned tasks, such as target capture or transportation relying on the robot-task-target matrices. For target transportation, the contact force acting on the target by each subteam robot is adjusted, which could cause the subteam robots to have a firm grip of the target.

SIMULATION RESULTS

In simulations, Sim (1) - Sim (3), as shown in Table 2, the SMMS control methods with and without the robot-task-target pairing method for homogeneous and heterogeneous robots were

simulated in the presence of time-varying communication delays to generate results for performance improvement. The simulated communication delay varied from 0 to 0.1 seconds randomly. The maximum communication delay of 0.1 second was chosen in the simulations because for the earth application, there is a critical value, beyond which the system tends to become unstable [2]. In the simulations, as shown in Figure 2(a), a master robot was a joystick connected to a laptop that read human operator motion commands and sent human commands to a virtual slave robot model . The virtual slave robot models in Figure 2(b) were programmed to execute the transmitted commands and/or generate and follow reference positions and velocities to perform the assigned tasks on the targets. In Sim (1) and (2), as shown in Figure 4, seven robots were simulated as holonomic mobile platforms, all of which has two active wheels, with a manipulator atop to form a team. In Sim (3), four of the team robots were with manipulators atop as shown in Figure 4 when the others were without manipulators atop as shown in Figure 3. Moreover, six virtual static obstacles and two virtual targets were modeled as mass-spring-damper systems [2]. All virtual obstacle, target, and robot positions and velocities were assumed to be known in the simulations. The two simple tasks, transportation and capture, were performed by the slave robots simultaneously. TB was transported by at least three mobile robots when TA was also captured by at least three mobile robots. TB was placed on a movable platform with four passive omni-directional wheels tightly touching the ground. There was no slip between the surfaces of the ground and the wheels. Besides, TA was fixed on the ground. It was captured while being encircled by the three mobile robots.

The simulations were set up with the following parameters. The desired safety distance between two robots was set to $3m$. The minimum distance between a robot and an obstacle was set

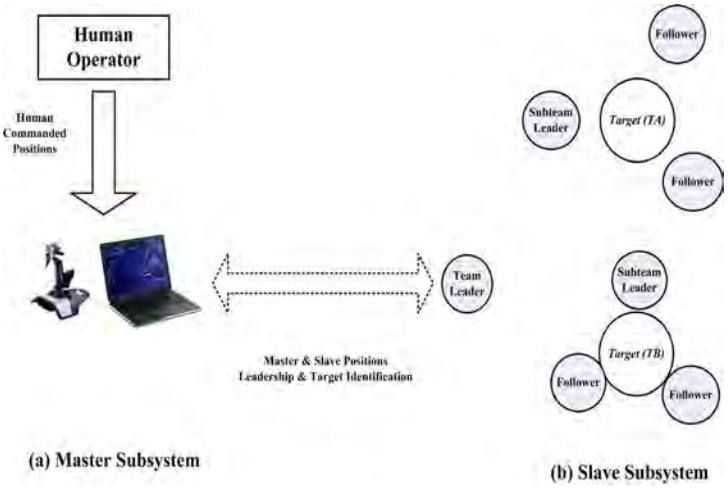

FIGURE 2: SMMS Simulation Setup

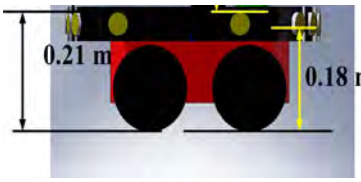

FIGURE 3: Mobile platform

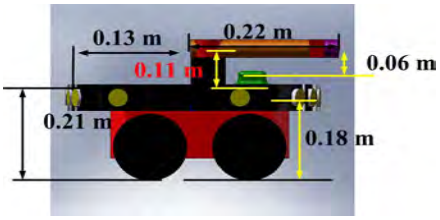

FIGURE 4: Mobile platform with the arm

to $5m$. Six circular objects with the radii of $5m$ were used as obstacles in each simulation. In the simulations, the six circular obstacles, Ob1-6, were situated at (30, 60), (50, 40), (70, 20), (70,-20), (50,-40), and (30,-60), respectively. Another two circular objects with the radii of $5m$ represented targets, TA and TB, in each simulation. TA and TB were initially static and situated at (90, 30) and (90, -30), respectively, as shown in Figures 5 and 9. The seven slave robots, R1-7, were initially located at (0, 15), (0, 10), (0, 5), (0, 0), (0, -5), (0, -10), and (0, -15), respectively. Only two directions parallel to the ground were considered in the simulations. Each slave robot was represented by a circular object with the radius of $3m$ in simulations. The slave robots with transporting TB were commanded to move from (90, -30) to (130, -30) in Figure. In the simulations, the following parameters were used:

M_m = 3 kg, K_m = 6 Ns/m, M_{si} = 30 kg, B_{si} = 1.0 Ns/m, K_{si} = 60 N/m, $/mu$ = 10, k_e = 100, b_e = 60, r_{imin} = 5, r_{smin} = 5, k_f = 1, α = ρ = 1, β_1 = 10000, β_0 = 500, ϕ = 100, and $\Lambda_i = \varphi = \gamma = \gamma_w$ =1

Simulation - Sim(1)

In Sim (1), the seven robots formed a team teleoperated by a human operator via the master robot. The human operator remotely controlled the team leader, R4, to reach TA, and all other slave robots, R1-3 and R5-7, were coordinated with the team leader to surround TA to capture it. After the TA capture, the human operator commanded the team leader, R4, to move to TB while other robots, R1-3 and R5-7, were also moving with regard to the team leader motion to approach TB. During the team navigations to catch TA and TB in Figure 5, all robots in the team were able to avoid the obstacles, Ob1-6 while the robots kept a constant distance from each other. As long as the team leader, R4, telecontrolled by the human operator had a contact with TB, the other robots, R1-3 and R5-7, encircled and contacted with it, and then all robots, R1-7, induced and regulated contact forces

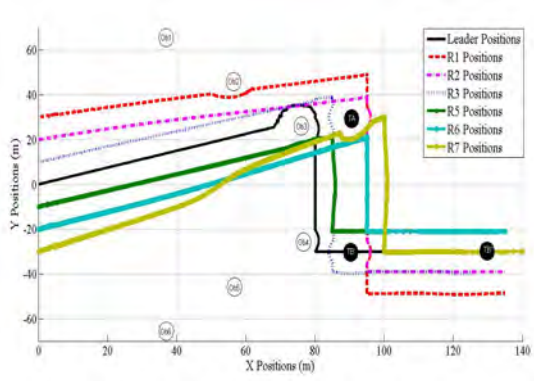

FIGURE 5: **Sim (1)** - Actual Path Trajectories

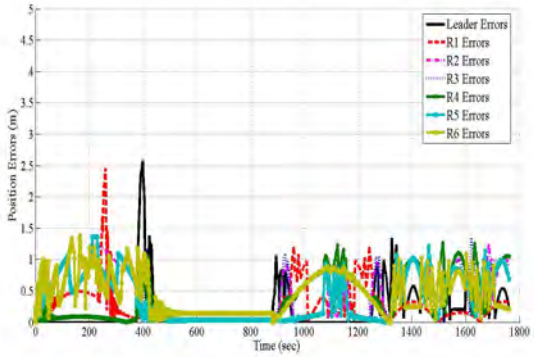

FIGURE 7: **Sim (1)** - Slave Position Errors

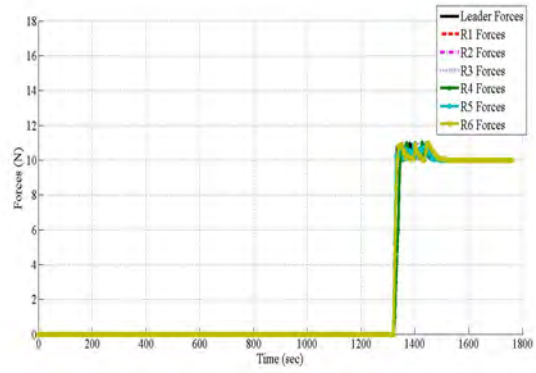

FIGURE 6: **Sim (1)** - Slave Forces

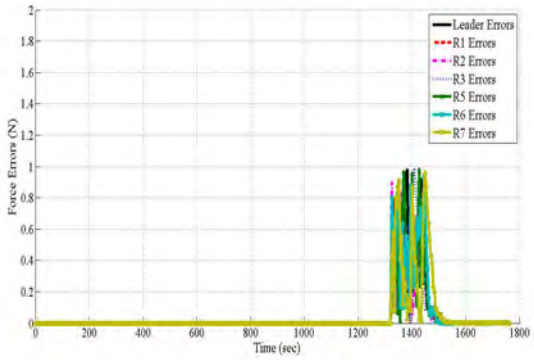

FIGURE 8: **Sim (1)** - Slave Force Errors

against it as shown in Figure 6 in order to have a firm grip of it. In Figure 5, TB was transported in 40(m) from (90, -30) to (130, -30), and Sim (1) was finished in 1760 seconds.

In Figures 6 and 8, the contact forces were maintained at 10 (N), when force errors δF_{si} varied between 1.0 and 0.0 (N), and its average was 0.65 (N), which was acceptable as mentioned above. The force errors were a little high due to the communication delays between the robots.

In Figures 7, position errors e_{si} of the team leader and R1-6 were presented, respectively. The position errors varied from 2.5 to 0 (m), which was mostly caused by the time-varying communication delays. The position error average, 0.65 (m), was still acceptable because the team leader robot teleoperated by the human operator moved slowly when the other robots, R1-3 and R5-6, moved with regard to the team leader positions.

Simulation - Sim(2)

In Sim (2), two tasks, Task 1, i.e. target transporting and Task 2, i.e. target capturing, were performed. The seven robots, R1-7, could form 35 types of Robot Combinations (Subteams (Sub1-35)) as shown in Table 3.

For Task 1, the desired contact forces were 8.0(N), and the target, TB, was moved from $(90,-30,0)$ to $(130,-30,0)$. For Task 2, the desired contact forces were 0(N), and the target, TA, was not moved because the task did not require the robot subteam to carry the target. With the robot-task-target pairing method mentioned in Eqs (1) - (5), the WAGT Tables were generated. Subteams (Sub1 - 35) and their bids for Task 1 (t_1) and Task 2 (t_2) were found for TA and TB in Table 4. Bids in Table 4, (Ta, Tb) where Ta is the bid value for TA when Tb is for TB, were calculated in Eq. (5) as an inverse of the sum of target-robot distances in a subteam minus the base price when the base price for t_1 was 30 and t_2 was 10. The reasons were that in order to start with the tasks, the robots needed to maintain at least 30(m) from TB for t_1 when only keeping at least 10(m) from TA for t_2 because the robots need more space to do t_1 than t_2.

As shown in Figure 9, only the team leader, R4, was teleoperated by the human operator when all other robots, R1-3 and R5-7, automatically formed two subteams, (R1-3 and R5-7 combinations) to capture TA and transport TB simultaneously in 1250 seconds, respectively. R4 was not engaged in any task, which

TABLE 3: Robot Combinations (Robot Subteams)

Subteam	Combos	Subteam	Combos	Subteam	Combos
Sub1	R1 R2 R3	Sub13	R1 R5 R6	Sub25	R2 R6 R7
Sub2	R1 R2 R4	Sub14	R1 R5 R7	Sub26	R3 R4 R5
Sub3	R1 R2 R5	Sub15	R1 R6 R7	Sub27	R3 R4 R6
Sub4	R1 R2 R6	Sub16	R2 R3 R4	Sub28	R3 R4 R7
Sub10	R1 R4 R5	Sub22	R2 R4 R7	Sub34	R4 R6 R7
Sub11	R1 R4 R6	Sub23	R2 R5 R6	Sub35	R5 R6 R7
Sub12	R1 R4 R7	Sub24	R2 R5 R7		

TABLE 4: Weighted Attack Guidance Table (WAGT) for Target A and B

Subteam	Bids	Subteam	Bids	Subteam	Bids
Sub1	(41,69)	Sub13	(39,73)	Sub25	(38,76)
Sub2	(40,69)	Sub14	(39,74)	Sub26	(39,74)
Sub3	(40,70)	Sub15	(38,75)	Sub27	(39,75)
Sub4	(40,71)	Sub16	(40,71)	Sub28	(39,75)
Sub10	(40,72)	Sub22	(39,74)	Sub34	(38,78)
Sub11	(39,73)	Sub23	(39,75)	Sub35	(38,79)
Sub12	(39,73)	Sub24	(39,75)		

could reduce the time delay effect on the task achievements. All tasks were done by the two subteams, Sub1 and Sub35, fully autonomously. In Figure 10, the simulation results showed that the contact forces were maintained at 10 (N) when the force errors, δF_{si}, varied from 0.0 to 0.9(N), and force error average was 0.45 (N) The position errors, e_{si}, varied from 0 to 0.12 (m) in Figures 11, and a position error average was 0.05 (m). The δF_{si} and e_{si} were caused by robotic path adaptation due to the modified potential field based formation control method and time-varying communication delays between the robots. By comparing those errors in Figures 11 and 12 and 7 and 8, the performance of the system in Sim (2) was better than that in Sim (1). The tasks were finished more quickly in 1250 seconds, and the position and force errors were smaller in Sim (2) for two reasons. (1) the amount of information transmitted over the time-varying links between the master and slave subsystems became less in Sim(2) than Sim(1) when only autonomous local slave robots handled the tasks, but the teleoperated R4 acted as a supervisor to monitor other robot

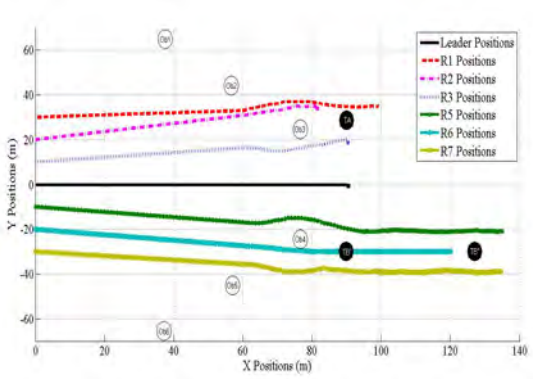

FIGURE 9: **Sim (2)** - Actual Path Trajectories

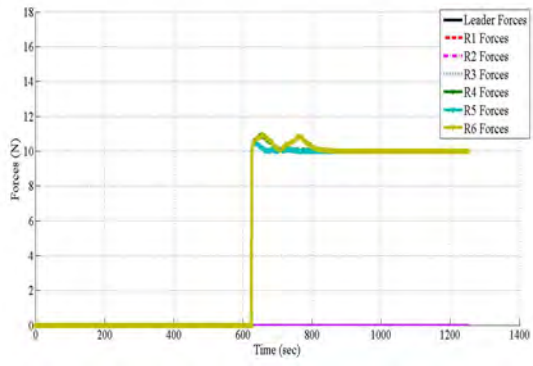

FIGURE 10: **Sim (2)** - Slave Forces

operations. (2) Forming the subteams could save all seven robots from visiting all targets to complete two tasks. The seven robots were split into three robots in one subteam to perform the task on each target simultaneously as shown in Figure 9. By taking advantage of the task planning independently done by each subteam, the task completion effectiveness was enhanced when the operation time was decreased to 1250 seconds in Sim(2) from 1760 seconds in Sim(1) in Figures 11 and 7 as the robot average speed was constant during the simulations.

Simulation - Sim(3)

In Sim (3), R1-3 were shown in Figure 4 when R4-7 were shown in Figure 3. The obstacles, targets, and tasks were equivalent to the ones specified in Sim (1-2). By solving Eqs. (6) within Eq. (7), Table 5 was generated. Therefore, Sub35 was paired to TA for the task of the target capture when Sub1 was paired to TB for the task of the target transportation, and R4 was a team leader.

In Figure 14, the simulation results showed that the contact forces were also maintained at 10 (N), which represented a firm grip of TB. Moreover, in Figure 16, the force errors varied from

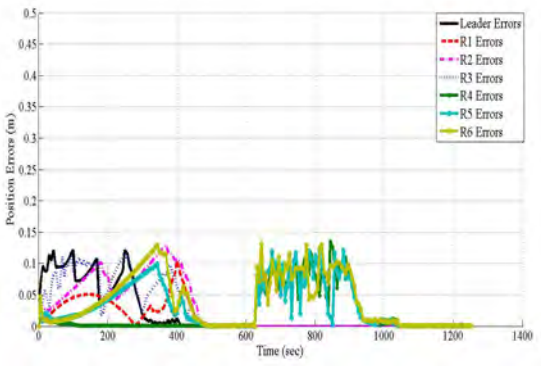

FIGURE 11: **Sim (2)** - Slave Position Errors

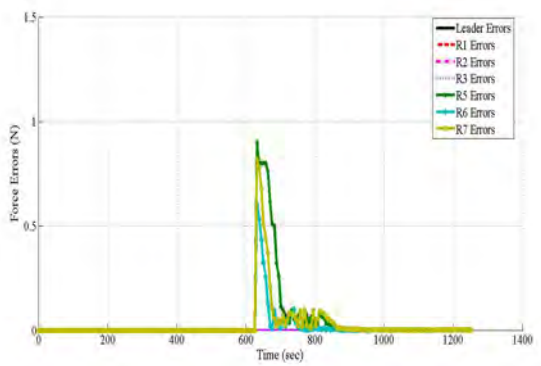

FIGURE 12: **Sim (2)** - Slave Force Errors

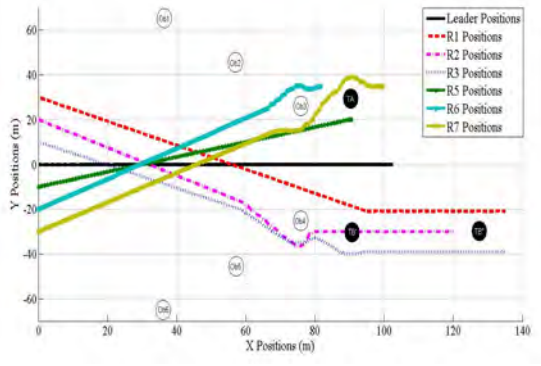

FIGURE 13: **Sim (3)** - Actual Path Trajectories

0.0 to 0.85(N), and their average was 0.25 (N) when in Figures 15, the position errors were recorded from 0 to 0.35 (m), and their average was 0.08 (m). By comparing the results in Sim(2) and Sim(3), their recorded force and position errors were similar, and their mission completion time was not quite different. Therefore, the performance of the proposed system was not affected by using the heterogeneous robots.

TABLE 5: Weighted Attack Guidance Table (WAGT) for Target A and B in Sim(3)

Subteam	Bids	Subteam	Bids	Subteam	Bids
Sub1	(41,369)	Sub13	(239,173)	Sub25	(238,176)
Sub2	(140,269)	Sub14	(239,174)	Sub26	(239,174)
Sub3	(140,270)	Sub15	(238,175)	Sub27	(239,175)
Sub4	(140,271)	Sub16	(240,171)	Sub28	(240,175)
Sub10	(240,172)	Sub22	(239,174)	Sub34	(328,178)
Sub11	(239,173)	Sub23	(239,175)	Sub35	(338,179)
Sub12	(239,173)	Sub24	(239,175)		

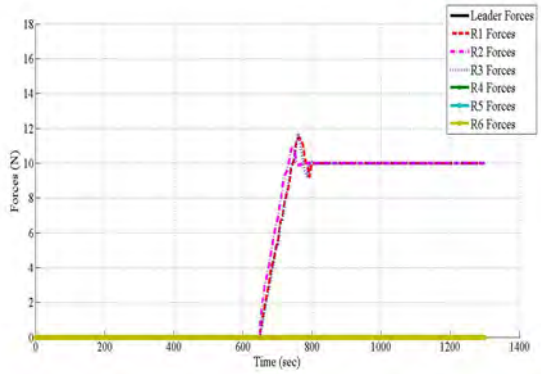

FIGURE 14: **Sim (3)** - Slave Forces

CONCLUSION & FUTURE WORK

The control method integrating the above mentioned main components is developed for the SMMS teleoperations to do the multi-task on the multi-target and improve the performance in terms of the effectiveness of the task achievement. Nonetheless, the proposed robot-task-target pairing method could generate a suboptimal solution in general since it is heuristic.

Therefore, our future work will be to further evaluate the performance of using the proposed robot-task-target pairing method to verify the performance and quality of the pair solutions. In addition, we will look into the proposed control method to team heterogeneous robots working in much complicated tasks and environments, e.g. an uncertain task that may include unconstrained, constrained, transition, or some motions combining two or all of them in an unknown area, which has not been seen in this paper.

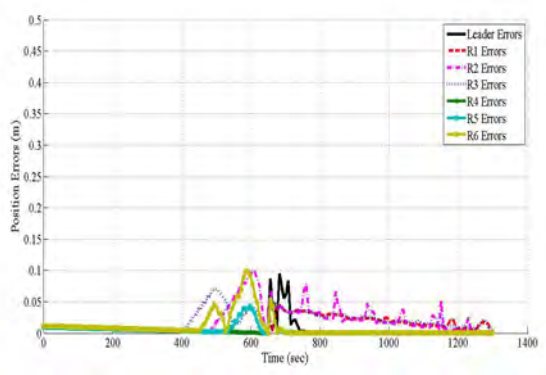

FIGURE 15: **Sim (3)** - Slave Position Errors

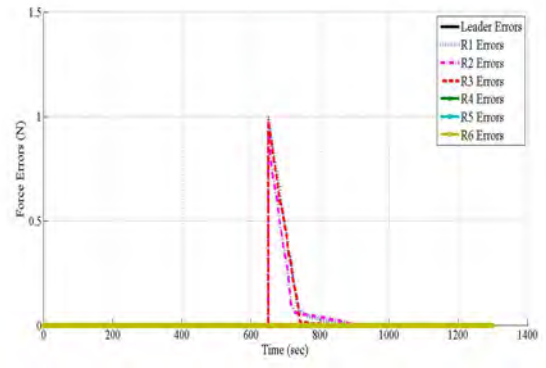

FIGURE 16: **Sim (3)** - Slave Force Errors

REFERENCES

[1] Z. R. Bogdanowicz and N. P. Coleman. New algorithm for optimization of effect-based weapon-target pairings. *International Conference Scientific Computing CSC 08*, 2008.

[2] Yushing Cheung. *Adaptive semi-autonomous teleoperation of a multi-agent robotic system*. PhD thesis, Stevens Institute of Technology, 2009.

[3] L. De-Lin, S. Chun-Lin, W. Biao, and W. Wen-Hai. Air combat decision-making for cooperative multiple target attack using heuristic adaptive genetic algorithm. *Machine Learning and Cybernetics, Proceedings of 2005 International Conference*, 1:473–478, 2005.

[4] M. B. Dias, R. M. Zlot, N. Kalra, and A. Stentz. Market-based multirobot coordination: a survey and analysis. *Proceedings of the IEEE*, 94(7):1257–1270, 2006.

[5] T. Fong, C. Thorpe, and C. Baur. Multi-robot remote driving with collaborative control. *Industrial Electronics, IEEE Transactions*, 50(4):699–704, 2003.

[6] K. Hashtrudi-Zaad and S.E. Salcudean. Adaptive transparent impedance reflecting teleoperation. *Proc. of the 1996 IEEE Int. Conf. Robotics and Automation*, 1996.

[7] Y. Kume, Y. Hirata, Zhi-Dong Wang, and K. Kosuge. Decentralized control of multiple mobile manipulators handling a single object in coordination. *Intelligent Robots and Systems, IEEE/RSJ International Conference*, 3:2758 – 2763, 2002.

[8] Dongjun Lee, O. Martinez-Palafox, and M.W. Spong. Bilateral teleoperation of multiple cooperative robots over delayed communication networks: Theory. *Robotics and Automation, ICRA. Proceedings of the IEEE International Conference*, 2005.

[9] Z. J. Lee, C. Y. Lee, and S. F. Su. An immunity-based ant colony optimization algorithm for solving weapontarget assignment problem. *Applied Soft Computing Journal*, 2(1):39–47, 2002.

[10] Bo Liu, Zheng Qin, Rui Wang, You bing Gao, and Li ping Shao. A hybrid heuristic particle swarm optimization for coordinated multi-target assignment. *Industrial Electronics and Applications, ICIEA. 4th IEEE Conference*, pages 1929 – 1934, 2009.

[11] L. Ni and D.W.L. Wang. Contact transition stability analysis for a bilateral teleoperation system. *Robotics and Automation 2002. Proceedings, ICRA '02*, 3(11-15):3272–3277, 2002.

[12] K. Ohba, S. Kawabata, N.Y. Chong, K. Komoriya, T. Matsumaru, N. Matsuhira, K. Takase, and K. Tanie. Remote collaboration through time delay in multiple teleoperation. *Intelligent Robots and Systems, 1999. IROS '99. Proceedings. 1999 IEEE/RSJ International Conference on*, 3:1866–1871, 1999.

[13] J Ota, N. Miyata, T. Arai, E. Yoshida, D. Kurabatashi, and J. Sasaki. Transferring and regrasping a large object by cooperation of multiple mobile robots. *Human Robot Interaction and Cooperative Robots, Proceedings. IEEE/RSJ International Conference*, 1995.

[14] A. Pongpunwattana and R. Rysdyk. Real-time planning for multiple autonomous vehicles in dynamic uncertain environments. *Journal of Aerospace Computing, Information, and Communication*, 1(12):580–604, 2004.

[15] T. Suzuki, T. Sekine, T. Fujii, H. Asama, and I. Endo. Cooperative formation among multiple mobile robot teleoperation in inspection task. *Decision and Control 2000, Proceedings of the 39th IEEE Conference*, 1(12-15):358–363, 2000.

[16] Z. Wang, M.N. Admadabadi, E. Nakano, and T. Takahashi. A multiple robot system for cooperative object transportation with various requirements on task performing. *Robotics and Automation, 1999. Proceedings. 1999 IEEE International Conference*, 2(10-15):1226–1233, 1999.

[17] Y. Yamamoto and S. Fukuda. Trajectory planning of multiple mobile manipulators with collision avoidance capability. *Proceedings. ICRA '02. IEEE International Conference*, 2002.